J Math Imaging Vis (2011) 40: 259–268
DOI 10.1007/s10851-011-0261-7

On the Occurrence Probability of Local Binary Patterns: A Theoretical Study

Francesco Bianconi · Antonio Fernández

Published online: 1 February 2011

Abstract It is well-known that local binary pattern (LBP) histograms of real textures exhibit a markedly uneven distribution, which is dominated by the so-called uniform patterns. The widely accepted interpretation of this phenomenon is that uniform patterns correspond to texture microfeatures, such as edges, corners, and spots. In this paper we present a theoretical study about the relative occurrence of LBPs based on the consideration that the LBP operator partitions the set of grayscale patterns into an ensemble of disjoint multidimensional polytopes. We derive exact prior probabilities of LBPs by calculating the volume of such polytopes. Our study puts in evidence that both the uneven distribution of the LBP histogram and the high occurrence of uniform patterns are direct consequences of the mathematical structure of the method rather than an intrinsic property of real textures.

Keywords Local binary patterns · Texture · Polytopes

1 Introduction

Texture analysis represents a fundamental building block of many computer vision and image processing applications. This research topic has received increasing attention during the last decades, and, consequently, many approaches have been proposed. Such a vast set of methods—which has been recently referred to as a "galaxy of texture features"—includes Julesz textons, Gabor filters, wavelets, Markov randon fields, co-occurrence matrices, Laws masks, texture spectrum, run lengths, trace transform and many others. Comprehensive surveys can be found in literature [27, 35, 39]. Within this galaxy the LBP has emerged as one of the most prominent techniques. The reasons of the success of this method are basically three: 1) easiness of implementation, 2) low computational overhead and 3) high discriminative power. Such characteristics make it an ideal candidate for many applications, including real-time processing. Since its introduction [25], the method has been successfully applied to many diverse areas of image processing: medical and biomedical image analysis [12, 24, 31], face and facial expression recognition [1, 11, 29], fingerprint matching [23], surface inspection and grading [9, 20, 33], remote sensing [18], motion analysis and object tracking [13, 34].

Despite its widespread adoption and the ample literature, little theoretical investigation has been carried out on this method. As a result some important questions still remain unresponded. One of the basic concerns is about the relative occurrence of local binary patterns. Many experimental results show that local binary patterns have a markedly uneven distribution in real textures [9, 15, 21, 26]. Such distribution seems to be dominated by the so called *uniform* patterns, namely those patterns whose number of bitwise 1/0 transitions (and vice versa) is at most two. Ojala et al. [26] reported a proportion of uniform patterns ranging from 76.6% to 91.8% in textures picked from the Brodatz database and from 82.4% to 93.3% in textures picked from the OuTex database. Recently a similar trend has been found by Liao et al. [15], who considered textures from the Brodatz, Meastex and CURet databases.

F. Bianconi (✉)
Dipartimento Ingegneria Industriale, Università degli Studi di Perugia, Via G. Duranti, 67, 06125 Perugia, Italy
e-mail: bianco@unipg.it

A. Fernández
Escuela de Ingeniería Industrial, Universidade de Vigo, Campus Universitario, 36310 Vigo, Spain
e-mail: antfdez@uvigo.es

So far the high incidence of uniform patterns has been explained in an "objective" way: they would be fundamental properties *of the observed textures* corresponding to primitive microfeatures such as corners, edges, and spots [26]. Herein we look at the problem from a different perspective and propose an alternative "subjective" explication: the high occurrence of uniform patterns might be an intrinsic characteristic *of the method* through which textures are analysed. In order to support this claim we take a closer look at the rationale behind the method from a mathematical standpoint. We determine the *exact* prior probabilities of local binary patterns under the assumption that the grayscale values are uncorrelated, and prove that the uniform patterns have high probability of occurrence. We propose to regard the LBP operator as a partition of the set of grayscale patterns into multidimensional polytopes. Following this approach, the prior probabilities of LBP patterns can be conveniently computed by calculating the volumes of such polytopes.

The remainder of the paper is organized as follows: Sect. 2 briefly recalls the basics of the LBP, Sect. 3 describes two alternative methods to evaluate the probability distribution in the case of the $LBP_{3\times3}$, Sect. 4 extends the evaluation to the case of the $LBP_{8,1}$, and Sect. 5 summarizes the main conclusions of the work.

2 The LBP Texture Model

Detailed descriptions of the LBP method can be found in various papers [19, 26]. Herein, in order to make the paper self-contained, we just recall the basic concepts of the method. The approach is based on the concept of local thresholding: a grayscale window $W = \{x_i \in \mathbb{N} : 0 \leq x_i \leq (N-1), i = 0, \ldots, n-1\}$, is converted into a set of binary values $B = \{b_i \in \{0,1\}, i = 1, \ldots, n-1\}$ through the following rule:

$$b_i(x_i, x_0) = \begin{cases} 1 & \text{when } x_i \geq x_0 \\ 0 & \text{when } x_i < x_0 \end{cases} \tag{1}$$

where n is the number of pixels in the window, N the number of grayscale values, x_0 the central pixel of the window, and $\mathbb{N}$ the set of nonnegative integers. Therefore the LBP defines a mapping from the space of all the possible N^n grayscale patterns formed by the n pixels of the window to the space of all the possible $2^{(n-1)}$ binary patterns that can be formed by the resulting binary values of the n pixels of the window but the central one. The histogram which quantifies the occurrence of such binary patterns represents the texture signature.

The original version of the LBP [25] is based on the $2^8 = 256$ possible binary patterns obtainable from a squared 3×3 window when thresholded by the value of the central pixel (Fig. 1). Each pattern can be uniquely identified through a string of eight binary numbers $b_8b_7b_6b_5b_4b_3b_2b_1$, which represent the pattern "code". Following the commonly accepted convention we refer to this method as the $LBP_{3\times3}$.

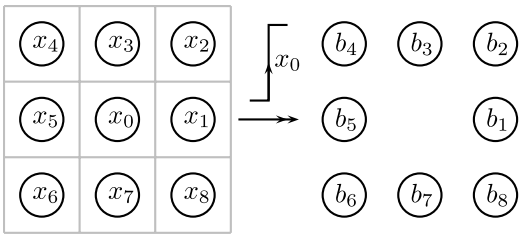

Fig. 1 The $LBP_{3\times3}$ texture model

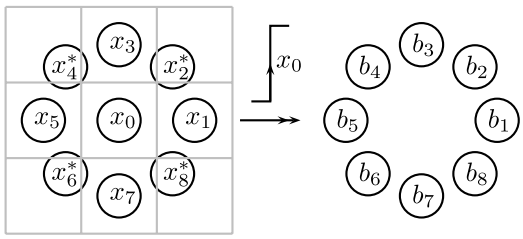

Fig. 2 The $LBP_{8,1}$ texture model. Interpolated values are marked with asterisks

Rotation-invariant versions of the method are obtained by grouping together all the binary patterns that are actually rotated versions of the same pattern. A preliminary step to obtaining rotation invariant versions consists in converting the original squared neighbourhood into a circular one. The gray values of the neighbours that do not coincide with the pixels centers are estimated through bilinear interpolation [19]. If we apply it to a 3×3 window we obtain the $LBP_{8,1}$ texture model (Fig. 2).

Having defined these two basic models, we can obtain extended versions by considering different radii of the interpolation circle and different angular spacing [26].

3 Relative Incidence of Local Binary Patterns: The Case of $LBP_{3\times3}$

In this section we derive a priori probabilities of local binary patterns for the $LBP_{3\times3}$ texture model. The case of the $LBP_{8,1}$ is analyzed in Sect. 4. Being interested in deriving a priori probabilities, we assume we are given no specific texture to analyse. This lack of knowledge can be modeled through a non-informative probability distribution. We make the following assumptions:

1. the grayscale values of the pixels in the neighbourhood are stochastically independent;
2. the grayscale value is uniformly distributed.

The assumption of uniform distribution is motivated by two reasons. First, since the main objective of the paper is to investigate the LBP method itself—regardless of the image it is applied to—we assume that no a priori information is given about the underlying image model. Such a situation is best modelled by a uniform distribution, which is the non-informative distribution *par excellence*. Secondly, a texture descriptor, as the LBP is, can be regarded to as a channel through which we convey information about the analysed image, where the pattern distribution is the output and the image is the input. Therefore studying the distribution of LBP is the same as studying the channel capacity. From information theory we know that the information processed by a channel (as defined in [2]) depends on the input distribution, which, in this case, represents the stochastic image model we use for our computations. We may vary the input distribution until the information processed by the channel attains a maximum: the channel capacity. In this sense the use of the uniform distribution as *universal prior* has been sustained by various authors, most remarkably by Shulman and Feder [30]. They show that the degradation of the mutual information with respect to the capacity when using the uniform distribution as a prior is minimal in many cases, and it is at most 6% of the channel capacity. Therefore, by using the uniform distribution as a prior, we expect to make the LBP work close to its theoretical capacity (i.e. not far from it more than 6%).

In the following computations we consider the grayscale value both as a continuous and as a discrete variable.

3.1 $LBP_{3\times3}$: The Continuous Case

The continuous case is actually a hypothetical scenario since most imaging systems are, nowadays, digital. Such ideal condition, however, is worth studying, since it represents a limit as the number of grayscale levels tends to infinity. In this case the grayscale intensity is a continuous variable uniformly distributed in $[0, 1]$: $\bar{x}_i \sim U[0, 1]$, $i \in \{0, \ldots, 8\}$. Throughout this paper we adopt the convention that the $\bar{}$ sign refers to continuous-valued variables. Moreover, in the following equations, the subscripts $_{3\times3}$ and $_{8,1}$ are used to tag variables referred to the $LBP_{3\times3}$ and $LBP_{8,1}$ texture models respectively.

For a given value $\bar{x}_0$ of the central pixel, the probability for one pixel of the neighbourhood to take binary value $b_v \in \{0, 1\}$ is:

$$\bar{p}_{3\times3}(b_v|\bar{x}_0) = \begin{cases} \bar{x}_0 & \text{when } b_v = 0 \\ 1 - \bar{x}_0 & \text{when } b_v = 1 \end{cases} \tag{2}$$

Under the assumptions stated at the beginning of Sect. 3 the probability of occurrence of an $LBP_{3\times3}$ pattern can be modeled as a repetition of independent trials with probabilities $\bar{x}_0$ for $b_v = 0$ and $(1 - \bar{x}_0)$ for $b_v = 1$. Consequently the a priori probability that a grayscale pattern maps to an $LBP_{3\times3}$ binary pattern, for a given value of $\bar{x}_0$, only depends on the total number of "0s" (or, equivalently, of "1s") that appear in it, and can be expressed as follows:

$$\bar{p}_{3\times3}(b_8b_7b_6b_5b_4b_3b_2b_1|\bar{x}_0) = \bar{x}_0^k(1 - \bar{x}_0)^{(8-k)} \tag{3}$$

where k is the total number of "0s" contained in the pattern binary string. Under the assumption that $\bar{x}_0 \sim U[0, 1]$, the a priori probability of a pattern is given by:

$$\bar{P}_{3\times3}(b_8b_7b_6b_5b_4b_3b_2b_1) = \int_0^1 \bar{x}_0^k(1 - \bar{x}_0)^{(8-k)} d\bar{x}_0 \tag{4}$$

which can be expressed in closed form:

$$\bar{P}_{3\times3}(b_8b_7b_6b_5b_4b_3b_2b_1) = \frac{k!(8-k)!}{9!} \tag{5}$$

The corresponding values are reported in Table 1 (note that $\bar{P}_{3\times3}(k) = \bar{P}_{3\times3}(8 - k)$ due to duality between 1s and 0s in a binary pattern). The histogram in Fig. 3 shows the a priori probability of each of the 256 binary patterns. In this and in the following histograms we use the convention that green bars indicate uniform patterns and red bars non-uniform patterns. We recall that uniform patterns are those patterns in which the number of bitwise transitions (1/0 and vice versa) is at most two, as formally defined in [26]. For instance the patterns 00000000 and 00010000 are uniform, since the number of bitwise transitions is zero and two, respectively. On the contrary the patterns 01010000 and 01001010 are non-uniform since the number of bitwise transitions is four and six, respectively.

Table 1 A priori probabilities of $LBP_{3\times3}$ patterns as a function of the number of "0s" (k)

k	0, 8	1, 7	2, 6	3, 5	4
$\bar{P}_{3\times3}$	$\frac{1}{9}$	$\frac{1}{72}$	$\frac{1}{252}$	$\frac{1}{504}$	$\frac{1}{630}$

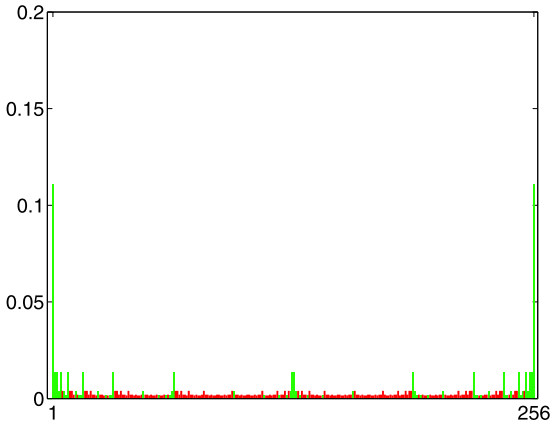

Fig. 3 A priori probabilities of $LBP_{3\times3}$ patterns in the continuous case

Table 2 A priori probabilities of $LBP_{3\times3}$ patterns as a function of N for given values of k

k	$P_{LBP_{3\times3}}(N)$
0	$\frac{1}{9} - \frac{1}{30N^8} + \frac{2}{9N^6} - \frac{7}{15N^4} + \frac{2}{3N^2} + \frac{1}{2N}$
1, 7	$\frac{1}{72} + \frac{1}{30N^8} - \frac{5}{36N^6} + \frac{7}{40N^4} - \frac{1}{12N^2}$
2, 6	$\frac{1}{252} - \frac{1}{30N^8} + \frac{5}{63N^6} - \frac{1}{20N^4}$
3, 5	$\frac{1}{504} + \frac{1}{30N^8} - \frac{11}{252N^6} + \frac{1}{120N^4}$
4	$\frac{1}{630} - \frac{1}{30N^8} + \frac{2}{63N^6}$
8	$\frac{1}{9} - \frac{1}{30N^8} + \frac{2}{9N^6} - \frac{7}{15N^4} + \frac{2}{3N^2} - \frac{1}{2N}$

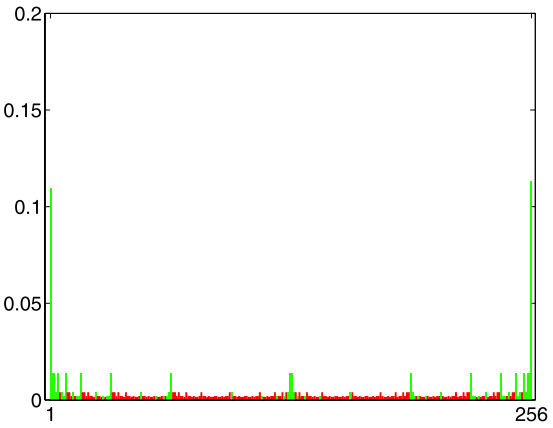

Fig. 4 A priori probabilities of $LBP_{3\times3}$ patterns in the discrete case, $N = 256$

3.2 $LBP_{3\times3}$: The Discrete Case

The formulas derived in Sect. 3.1 can be easily extended to the discrete case. For a given value x_0 of the central pixel, the probability for one pixel of the neighbourhood to get a binary value $b_v \in \{0, 1\}$ is:

$$p(b_v|x_0) = \begin{cases} \frac{x_0}{N} & \text{when } b_v = 0 \\ 1 - \frac{x_0}{N} & \text{when } b_v = 1 \end{cases} \quad (6)$$

Again, under the assumption that $x_0 \sim U[0, (N-1)]$, the a priori probability of a pattern is:

$$P_{3\times3}(b_8b_7b_6b_5b_4b_3b_2b_1) = \frac{1}{N^9} \sum_{x_0=0}^{N-1} {x_0}^k \, (N - x_0)^{(8-k)} \quad (7)$$

We can expand (7) to get the probabilities as a function of N for given values of k (see Table 2). As one would expect such expressions tends to the results obtained in the continuous case as $N \to \infty$. The histogram in Fig. 4 shows the probability of occurrence of each of the 256 binary patterns in the discrete case for $N = 256$.

We notice that both in the discrete and continuous case the most probable patterns are the flat area black/white spots (all bits "0" or "1", respectively). In the continuous case the distribution is perfectly symmetric, as one would expect (Fig. 3). In the discrete case, due to the $\geq$ in the LBP definition (1), the white spot pattern is slightly more probable than its black counterpart (Table 2, Fig. 4).

3.3 LBP as a Space Partitioning Method

In Sects. 3.1 and 3.2 we derived simple expressions for the a priori probabilities of $LBP_{3\times3}$ patterns using elementary statistical considerations. In this specific case our task is made easy by the relatively simple structure of the $LBP_{3\times3}$ model. With a more complicated model (e.g., $LBP_{8,1}$), however, similar expressions are very hard to find. Therefore in this section we describe an approach which makes it possible to deal with the problem in a more general way. We observe that the LBP operator can be interpreted as a *mapping* from the *grayscale* pattern space to the *binary* pattern space (Fig. 5). As detailed below, such mapping is defined through a partition of the grayscale pattern space. We would like to emphasize that local binary patterns should not be considered as physical entities. They are actually a way to mathematically formalize the partition of the grayscale pattern space.

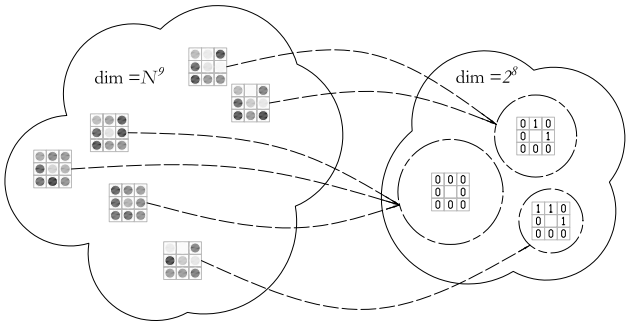

Fig. 5 The LBP model defines a mapping from the grayscale pattern space (*left*) to the binary pattern space (*right*)

Let's consider, first, the continuous case. In this scenario the grayscale pattern space is the 9-dimensional unit hypercube, and a grayscale pattern is just a point of the hypercube. The set of all the possible $LBP_{3\times3}$ patterns introduces a partition of the hypercube, each part $\bar{\mathcal{P}}$ being defined as follows:

$$\bar{\mathcal{P}}_{3\times3}(b_8b_7b_6b_5b_4b_3b_2b_1) = \left\{ \bar{\mathbf{x}} \in \mathbb{R}^9 : 0 \leq \bar{x}_i \leq 1, \quad \mathbf{A}\bar{\mathbf{x}} \geq \mathbf{0} \right\} \quad (8)$$

Binary code		
00000000	00000101	00001101

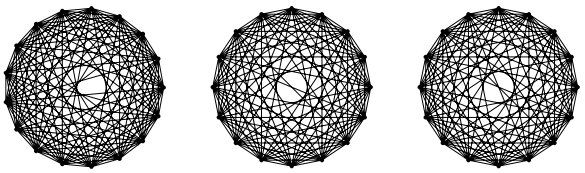

Fig. 6 The graph structure of the polytopes corresponding to the $LBP_{3\times3}$ patterns 00000000, 00000101, and 00001101

where:

$$\mathbf{A} = \begin{pmatrix} A_{10} & A_{11} & 0 & 0 & \cdots & 0 \\ A_{20} & 0 & A_{22} & 0 & \cdots & 0 \\ \cdots & \cdots & \cdots & \cdots & \cdots & \cdots \\ A_{80} & 0 & 0 & 0 & \cdots & A_{88} \end{pmatrix}; \tag{9}$$

$$A_{ij} = \begin{cases} 1 & \text{when } b_i = 0, \\ -1 & \text{when } b_i = 1, \end{cases} \quad j = 0, \qquad \begin{cases} -1 & \text{when } b_i = 0, \\ 1 & \text{when } b_i = 1, \end{cases} \quad j \neq 0; \tag{10}$$

$$\bar{\mathbf{x}} = \begin{pmatrix} \bar{x}_0 \\ \bar{x}_1 \\ \cdots \\ \bar{x}_8 \end{pmatrix}; \tag{11}$$

and $\mathbf{0}$ denotes a vector whose components are all 0.

This set of inequalities is usually referred to as the hyperplane description of a *polytope* in $\mathbb{R}^9$ [5]. Therefore the problem of computing the a priori probabilities of LBP patterns is the same as computing the volumes of the corresponding polytopes which partition the 9-dimensional unit hypercube. To get an idea of the "shape" of the polytopes which correspond to each $LBP_{3\times3}$ pattern we can plot their graph structure. This is the set of the 0- and 1-dimensional faces (vertices and edges) of the polytope. Higher dimensional faces are not considered in the graph. Figure 6 reports the graphs of three polytopes as example. The images have been obtained through the `Mathematica` implementation[1] of the Avis-Fukuda algorithm [3].

Efficient algorithms exist to compute the *exact* volume of polytopes. Herein we used `polymake` [10], a library for polytopes manipulation whose algorithm for volume calculation is based on Fukuda's `cddlib` implementation of the double description method of Motzkin et al. [22]. Through this library we could verify that the volumes of the polytopes coincide with the results reported in Table 1.

[1] http://library.wolfram.com/infocenter/MathSource/440/.

In the discrete domain the same line of reasoning leads to the problem of counting the number of integer points in a polytope [5, 32]. Consider a generic convex polytope $\mathcal{P}$:

$$\mathcal{P} = \{\mathbf{x} \in \mathbb{N}^n : x_i \geq 0, \mathbf{A}\mathbf{x} + t\mathbf{b} \geq \mathbf{0}\} \tag{12}$$

where $\mathbf{A}$ is an integral matrix, $\mathbf{b}$ an integer vector, t an integer parameter, and $\mathbf{x}$ is the discrete version of $\bar{\mathbf{x}}$ (11). In the above expression the elements of $\mathbf{b}$ represents the upper limits of the x_i, and so the effect of t is that of "inflating"/"deflating" the polytope. The number of integer points $L_{\mathcal{P}}(t)$ in $\mathcal{P}$ as a function of t is a polynomial in t of degree n when $\mathcal{P}$ is an *integer* polytope, and a quasi-polynomial of the same degree when $\mathcal{P}$ is a *rational* polytope [5, 8, 32]. These two results are usually referred to as the Ehrhart's theorem and the Ehrhart's theorem for rational polytopes, after French mathematician Eugéne Ehrhart, who first inaugurated the study of this problem.

A polytope as expressed in (12) is referred to as a *closed* polytope, since it is defined by closed half-spaces, being all the inequalities in (12) loose inequalities. In the case of the $LBP_{3\times3}$ it results, from the definition (1), that the polytope corresponding to a specific pattern is a *semi-open* polytope [36], since it is defined both by open and closed half-spaces. A semi-open polytope is a closed polytope minus some of its faces. To get an idea of this we can consider, for instance, a square minus some of its edges, or a cube minus some of its faces. A semi-open polytope can be expressed as follows:

$$\mathcal{P}_{3\times3}(b_8b_7b_6b_5b_4b_3b_2b_1) = \left\{\mathbf{x} \in \mathbb{N}^9 : 0 \leq x_i \leq (N-1), \quad \begin{matrix} \mathbf{A}'\mathbf{x} \geq \mathbf{0} \\ \mathbf{A}''\mathbf{x} > \mathbf{0} \end{matrix}\right\} \tag{13}$$

where $\mathbf{A}'$ and $\mathbf{A}''$ are integral matrices. The two inequalities that appear in the above equation have the following meaning: they represent the set of closed ($\mathbf{A}'\mathbf{x} \geq \mathbf{0}$) and open ($\mathbf{A}''\mathbf{x} > \mathbf{0}$) half spaces which define the polytope. Now from [36] (proposition 27) we derive that $\{\mathbf{x} \in \mathbb{N}^d : \mathbf{A}\mathbf{x} > \mathbf{0}\} = \{\mathbf{x} \in \mathbb{N}^d : \mathbf{A}\mathbf{x} - \mathbf{1} \geq \mathbf{0}\}$, where $\mathbf{1}$ is a vector whose components are all 1. Now we can convert the polytope in (13) into the following equivalent representation:

$$\mathcal{P}_{3\times3}(b_8b_7b_6b_5b_4b_3b_2b_1) = \left\{\mathbf{x} \in \mathbb{N}^9 : 0 \leq x_i \leq (N-1), \quad \mathbf{A}\mathbf{x} + \mathbf{c} \geq 0\right\} \tag{14}$$

where $\mathbf{A}$ is the same as in (10) and $\mathbf{c}$ is an 8×1 array whose elements are:

$$c_i = \begin{cases} -1 & \text{when } b_i = 0 \\ 0 & \text{when } b_i = 1 \end{cases} \tag{15}$$

In practice $\mathbf{c}$ is a slack variable which permits to treat both strict and non strict inequalities in the same way: the

Table 3 Number of lattice points inside $LBP_{3\times3}$ polytopes as a function of the number of levels N, for given values of k

k	$L(\mathcal{P}_{3\times3}(N))$
0	$\frac{1}{9}(N-1)^9+\frac{3}{2}(N-1)^8+\frac{26}{3}(N-1)^7+28(N-1)^6+\frac{833}{15}(N-1)^5+70(N-1)^4+\frac{506}{9}(N-1)^3+28(N-1)^2+\frac{239}{30}(N-1)+1$
1, 7	$\frac{1}{72}(N-1)^9+\frac{1}{8}(N-1)^8+\frac{5}{12}(N-1)^7+\frac{7}{12}(N-1)^6+\frac{7}{40}(N-1)^5-\frac{7}{24}(N-1)^4-\frac{5}{36}(N-1)^3+\frac{1}{12}(N-1)^2+\frac{1}{30}(N-1)$
2, 6	$\frac{1}{252}(N-1)^9+\frac{1}{28}(N-1)^8+\frac{1}{7}(N-1)^7+\frac{1}{3}(N-1)^6+\frac{9}{20}(N-1)^5+\frac{1}{4}(N-1)^4-\frac{11}{126}(N-1)^3-\frac{5}{42}(N-1)^2-\frac{1}{105}(N-1)$
3, 5	$\frac{1}{504}(N-1)^9+\frac{1}{56}(N-1)^8+\frac{1}{14}(N-1)^7+\frac{1}{6}(N-1)^6+\frac{31}{120}(N-1)^5+\frac{7}{24}(N-1)^4+\frac{13}{63}(N-1)^3+\frac{1}{42}(N-1)^2-\frac{4}{105}(N-1)$
4	$\frac{1}{630}(N-1)^9+\frac{1}{70}(N-1)^8+\frac{2}{35}(N-1)^7+\frac{2}{15}(N-1)^6+\frac{1}{5}(N-1)^5+\frac{1}{5}(N-1)^4+\frac{52}{315}(N-1)^3+\frac{16}{105}(N-1)^2+\frac{8}{105}(N-1)$
8	$\frac{1}{9}(N-1)^9+\frac{1}{2}(N-1)^8+\frac{2}{3}(N-1)^7-\frac{7}{15}(N-1)^5+\frac{2}{9}(N-1)^3-\frac{1}{30}(N-1)$

strict inequality $-x_i + x_0 > 0$ is converted into the equivalent loose inequality $-x_i + x_0 - 1 \geq 0$. In order to provide the interested reader with a greater insight into the notation, we report *in extenso* the matrices $\mathbf{A}$ and $\mathbf{c}$ for a specific pattern. If we consider, for instance the $LBP_{3\times3}$ pattern 00000101, we have:

$$\mathbf{A} = \begin{pmatrix} -1 & 1 & 0 & 0 & 0 & 0 & 0 & 0 & 0 \\ 1 & 0 & -1 & 0 & 0 & 0 & 0 & 0 & 0 \\ -1 & 0 & 0 & 1 & 0 & 0 & 0 & 0 & 0 \\ 1 & 0 & 0 & 0 & -1 & 0 & 0 & 0 & 0 \\ 1 & 0 & 0 & 0 & 0 & -1 & 0 & 0 & 0 \\ 1 & 0 & 0 & 0 & 0 & 0 & -1 & 0 & 0 \\ 1 & 0 & 0 & 0 & 0 & 0 & 0 & -1 & 0 \\ 1 & 0 & 0 & 0 & 0 & 0 & 0 & 0 & -1 \end{pmatrix}; \quad (16)$$

$$\mathbf{c} = \begin{pmatrix} 0 \\ -1 \\ 0 \\ -1 \\ -1 \\ -1 \\ -1 \\ -1 \end{pmatrix}$$

It has been shown that Ehrhart's results also hold for semi-open polytopes [36]. We also observe that the polytope in (14) can be treated as a *parametric* polytope of parameter $(N-1)$, according to the definition given by Clauss and Loechner [7].

Counting integer points in polytopes is difficult. When the dimension is an input variable the problem of detecting a lattice point in polyhedra is NP-hard [16]. Fortunately in 1993 Barvinok found an algorithm to count integer points inside polyhedra which runs in polynomial time provided that the dimension is fixed [4]. Later on the method has been extended to parametric polytopes [7], which is the case studied here. The Barvinok's algorithm and its extensions represent the basis of some free libraries to count integer points in polytopes such as `barvinok` [38] and `LattE` [17].

To compute the number of lattice points inside the polytope in (8), we used the `barvinok_ enumerate` program of the `barvinok` library, which enumerates the number of lattice points in a polytope as a piecewise step-polynomial. First of all we observe that the coordinates of the vertices of the polytope in (14) can take values 0 or 1, and therefore the polytope is integral. Consequently we expect the number of integer points in the polytope to be a polynomial in $(N-1)$ of degree 9. The results reported in Table 3 confirm that the number of integer points is indeed a polynomial in $(N-1)$ of degree 9. Now we can compute the probability of occurrence of each $LBP_{3\times3}$ pattern by dividing the number of lattice points in each corresponding polytope by the total number of points in the 9-dimensional hypercube (N^9). This leads to the same results reported in Table 2.

4 Relative Incidence of Local Binary Patterns: The Case of $LBP_{8,1}$

In this section we are concerned with the a priori distribution of local binary patterns when the original 3×3 window is converted into a circular lattice through bilinear interpolation. This is a preliminary step to make the method robust against rotation. The basic idea is that, as the texture rotates, the gray values of the neighbourhood move along the circle centered on the central pixel. The resulting model is referred to as the $LBP_{8,1}$ [19, 26]. We remark, beforehand, that converting from a squared neighbourhood to a circular one introduces an artificial dependence between the gray values which forces the interpolated points to take gray values "similar" to those of their neighbourhoods. As a consequence one can reasonably expect a significant change in the probability distribution, with a higher occurrence of uniform patterns.

In the $LBP_{8,1}$ model the interpolated points have coordinates $(\pm\sqrt{2}/2, \pm\sqrt{2}/2)$. Therefore the bilinearly interpolated gray value x_i^* is [28]

$$x_i^* = w_1 x_{\mathrm{mod}(i-1,8)} + w_2 x_i + w_1 x_{\mathrm{mod}(i+1,8)} + w_3 x_0 \quad (17)$$

where $i = 2, 4, 6, 8$ (Fig. 2), and:

$$\begin{aligned} w_1 &= (\sqrt{2}-1)/2 \\ w_2 &= 1/2 \\ w_3 &= (1-\sqrt{2}/2)^2 \end{aligned} \quad (18)$$

In this case no such simple formulas as in the case of the $LBP_{3\times3}$ can be found. Nonetheless, having established the equivalence between local binary patterns and space partitions, we can still compute the *exact* a priori probabilities through the polytope approach. For this approach to be applied, however, we have to make another assumption. From (17) and (18) it is evident that, in general, $LBP_{8,1}$ polytopes are *irrational*. Unfortunately there is still no theory to deal with this class of polytopes [5]. Therefore we consider rational approximations of the weights w_1, w_2 and w_3 which result from the assumption

$$\sqrt{2} \approx \frac{99}{70} \quad (19)$$

We believe that the above approximation, which is correct up to the fourth decimal digit, has very little effect on the estimation of the relative occurrence of $LBP_{8,1}$ patterns.

4.1 $LBP_{8,1}$: The Continuous Case

As in the case of $LBP_{3\times3}$ the set of all the possible $LBP_{8,1}$ patterns introduces a partition of the 9-dimensional hypercube, each part being defined as in (8), where, in this case the matrix $\mathbf{A}$ takes the following form:

$$\begin{pmatrix} A_{10} & A_{11} & 0 & 0 & 0 & 0 & 0 & 0 & 0 \\ A_{20}r_3 & A_{21}r_1 & A_{22}r_2 & A_{23}r_1 & 0 & 0 & 0 & 0 & 0 \\ A_{30} & 0 & 0 & A_{32} & 0 & 0 & 0 & 0 & 0 \\ A_{40}r_3 & 0 & 0 & A_{43}r_1 & A_{44}r_2 & A_{45}r_1 & 0 & 0 & 0 \\ A_{50} & 0 & 0 & 0 & 0 & A_{55} & 0 & 0 & 0 \\ A_{60}r_3 & 0 & 0 & 0 & 0 & A_{65}r_1 & A_{66}r_2 & A_{67}r_1 & 0 \\ A_{70} & 0 & 0 & 0 & 0 & 0 & 0 & A_{77} & 0 \\ A_{80}r_3 & A_{81}r_1 & 0 & 0 & 0 & 0 & 0 & A_{87}r_1 & A_{88}r_2 \end{pmatrix} \quad (20)$$

where the A_{ij} are defined as in (10). Now, bringing together (17)–(19), we get the following values for the integer coefficients r_1, r_2 and r_3:

$$\begin{aligned} r_1 &= 4060 \\ r_2 &= 9800 \\ r_3 &= 17919 \end{aligned} \quad (21)$$

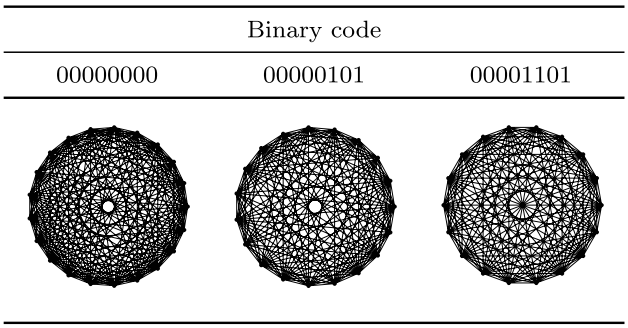

Fig. 7 The graph structure of the polytopes corresponding to the $LBP_{8,1}$ patterns 00000000, 00000101, and 00001101

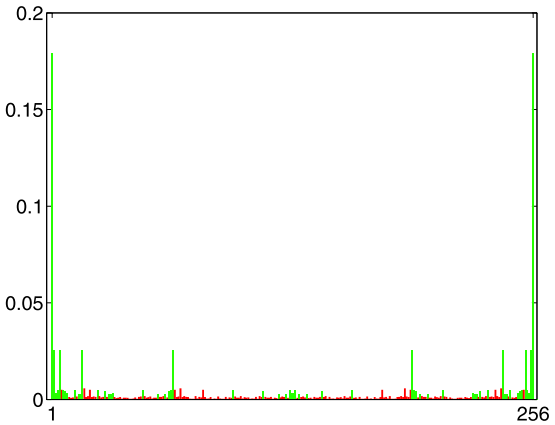

Fig. 8 A priori probabilities of $LBP_{8,1}$ patterns in the continuous case

As we did in Sect. 3.3 we report the graph structure of three $LBP_{8,1}$ polytopes (Fig. 7). In this case we notice that the structures are more complicated than the $LBP_{3\times3}$ counterparts (Fig. 6), which agrees with the difference in complexity between (9) and (20). The histogram of the a priori probability distribution of $LBP_{8,1}$ patterns in the continuous case is showed in Fig 8. Table 4 reports the exact values for the three local binary patterns of Fig. 7.

4.2 $LBP_{8,1}$: The Discrete Case

The discrete case can be solved through the same approach used for the $LBP_{3\times3}$ (Sect. 3.3). In particular (14) and (15) still hold, provided that we take the matrix $\mathbf{A}$ as in (20).

Table 5 reports the exact a priori probabilities of the three polytopes shown in Fig. 7. Looking at Figs. 8 and 9 we notice that the probability distribution changes significantly if compared with the 3×3 model. It is evident, in particular, the higher occurrence of the uniform patterns, as detailed in the following section.

4.3 The Contribution of Uniform Patterns

In the preceding sections we have described an approach to compute the exact a priori probability distributions of

Table 4 Exact a priori probabilities of the three $LBP_{8,1}$ patterns of Fig. 7 in the continuous case under the assumption of rational interpolation weights (18) and (19)

Pattern code	Probability
00000000	$\frac{3447468912735560803553827320929330000229406832026905543972301814386906130677847 27}{1924081986089385261773791551406115480477713193229373977028341133578240000000000000} \approx 0.1792$
00000101	$\frac{4331646668930993915197898019330214301838704365599522579379145782176708 1}{8646448079435116482887105528934777284707283437856410263796838400000000000} \approx 0.0050$
00001101	$\frac{1300207724501330515013291452255545892356869629130457894917521521545741 9}{8646448079435116482887105528934777284707283437856410263796838400000000000} \approx 0.0015$

Table 5 Exact a priori probabilities of the three $LBP_{8,1}$ patterns of Fig. 7 as a function of the number of levels N under the assumption of rational interpolation weights (18) and (19)

N	Pattern code		
	00000000	00000101	00001101
64	$\frac{3118238338969334}{64^9} \approx 0.1731$	$\frac{96258479582765}{64^9} \approx 0.0053$	$\frac{27692362324755}{64^9} \approx 0.0015$
128	$\frac{1624469658107347992}{128^9} \approx 0.1761$	$\frac{47735995000052987}{128^9} \approx 0.0052$	$\frac{14024790442690437}{128^9} \approx 0.0015$
256	$\frac{838907467027119809606}{256^9} \approx 0.1756$	$\frac{24045568889514282403}{256^9} \approx 0.0051$	$\frac{7141375193636033373}{256^9} \approx 0.0015$

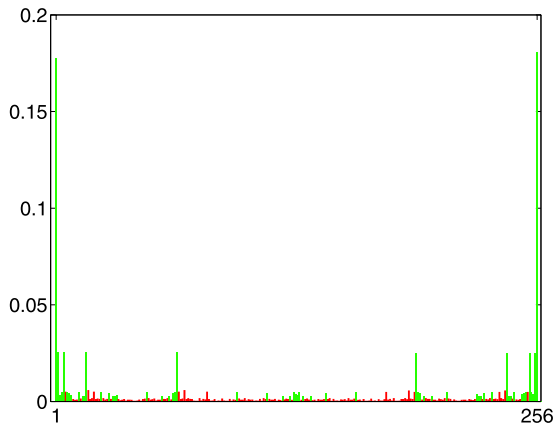

Fig. 9 A priori probabilities of $LBP_{8,1}$ patterns in the discrete case, $N = 256$

Table 6 Incidence of uniform patterns in the $LBP_{3\times3}$ and $LBP_{8,1}$ texture models

N	% of uniform patterns	
	$LBP_{3\times3}$	$LBP_{8,1}$
3	56.59198	70.08078
4	55.68389	72.38006
5	55.42405	73.18850
6	55.32865	73.89334
7	55.28726	74.36096
...	...	...
64	55.23810	74.87518
128	55.23809	74.88386
256	55.23809	74.88574
∞	55.23809	74.88667

$LBP_{3\times3}$ and $LBP_{8,1}$ patterns both in the continuous and discrete case. We can now compute the exact incidence of uniform patterns in these two models. In Table 6 we report the percentage of occurrence of uniform patterns for the two texture models in the discrete case (for different values of N) and in the continuous case.

The results reported in Table 6 put in evidence the high a priori probability of uniform patterns. In the case of the $LBP_{3\times3}$ such probability is about 55%. This value rises to about 75% in the case of the $LBP_{8,1}$. Such results suggest that the high occurrence of uniform patterns reported in literature may be a direct outcome of the intrinsic structure of the method. The results also confirm our guess that bilinear interpolation produces a significant increase of the percentage of uniform patterns.

5 Conclusions and Future Work

In this work we presented a theoretical study about the occurrence probability of local binary patterns. As noticed by various authors, such distribution is highly uneven in real textures, and seems to be dominated by the so-called uniform patterns. Based on this evidence, we decided to investigate whether such result should be considered a fundamental

property of real textures or something that logically follows from the mathematical structure of the method. In order to answer this question we developed an approach to evaluate the a priori statistical distribution of local binary patterns. The procedure is based on the consideration that the LBP can be interpreted as a space partitioning method. As a consequence the a priori probability of each pattern depends on the volume of the part it belongs to. We showed that these parts are polytopes in the 9-dimensional space, and therefore the a priori probabilities can be computed as the volume of polytopes (continuous case) or the number of lattice points inside a polytope (discrete case).

The results show that the a priori probability of uniform patterns is rather high: ≈55% in the case of the $LBP_{3\times3}$. This value increases significantly when the squared neighbourhood is converted into a circular one through interpolation, and reaches ≈75% in the case of the $LBP_{8,1}$. This result makes sense, since bilinear interpolation forces the interpolated pixels to take grayscale values similar to those of their neighbours. In the introduction we mentioned that other authors reported, with $LBP_{8,1}$, an incidence of uniform patterns ranging from 76.6% to 93.3% in real textures. If we compare these values with the theoretical value of ≈75% derived herein, we notice that the incidence of uniform patterns is even higher in real textures. This additional proportion of uniform patterns can be easily explained considering that the theoretical values have been computed under the assumption that grayscale values of adjacent pixels are uncorrelated. In real images it is often observed that pixels at nearby locations tend to have similar intensity values [6]. This results in an higher incidence of uniform patterns, since bitwise 1/0 transitions in the peripheral pixels are less probable than in the theoretical case.

As a general conclusion we can say that the high occurrence of uniform binary patterns is, to a great extent, a direct consequence of the inherent structure of the method. The highly uneven a priori distribution of local binary patterns might also be a drawback of the method itself, at least from a theoretical standpoint, for if we consider each possible pattern a symbol of an alphabet, the efficiency is maximum when all the symbols are equally likely.

An interesting by-product of the investigation proposed in this paper is the interpretation of the LBP as a space partitioning method. In our opinion the contribution of this is twofold: on the one hand we notice that other methods, such as, for instance, the ILBP [14] and the Image Patch-Based Classifiers [37] are based on the same idea, and therefore can be studied using the same strategy. On the other hand we believe that the idea of space partitioning can pave the way for the development of new texture descriptors, since the overall problem can be restated in a different way. Future research, in fact, might be focused on studying functions that map grayscale patterns into a lower dimensional space under the constraint that this mapping maximizes the theoretical amount of information that can be conveyed and it is invariant against rotation, grayscale changes or other transformations.

Acknowledgements This work was partially supported by a joint research programme among *Mondial Marmi SpA* (Perugia, Italy); *Dipartimento Ingegneria Industriale* (Università degli Studi di Perugia, Italy) and *Ministero dell'Istruzione dell' Università e della Ricerca* under the framework specified by the Ministerial Decree No. 593 of 8 August 2000. The authors would also like to thank the anonymous reviewers for their fruitful remarks.

References

1. Ahonen, T., Hadid, A., Pietikäinen, M.: Face description with local binary patterns: Application to face recognition. IEEE Trans. Pattern Anal. Mach. Intell. **28**, 2037–2041 (2006)
2. Ash, R.B.: Information Theory. Dover, New York (1965)
3. Avis, D., Fukuda, K.: A pivoting algorithm for convex hulls and vertex enumeration of arrangements and polyhedra. Discrete Comput. Geom. **8**, 295–313 (1992)
4. Barvinok, A.I.: Polynomial time algorithm for counting integral points in polyhedra when the dimension is fixed. Math. Oper. Res. **19**, 769–779 (1994)
5. Beck, M., Robins, S.: Computing the Continuous Discretely. Integer-Point Enumeration in Polyhedra. Springer, Berlin (2007)
6. Bovik, A.C.: Handbook of Image and Video Processing, 2nd edn., p. 432. Elsevier, Amsterdam (2005)
7. Clauss, P., Loechner, V.: Parametric analysis of polyhedral iteration spaces. J. VLSI Signal Process. **19**, 179–194 (1998)
8. Diaz, R., Robins, S.: The Ehrhart plynomial of a lattice polytope. Ann. Math. **145**, 503–518 (1997)
9. Fernández, A., Ghita, O., González, E., Bianconi, F., Whelan, P.F.: Evaluation of robustness against rotation of LBP, CCR and ILBP features in granite texture classification. Mach. Vis. Appl. (2010). doi:10.1007/s00138-010-0253-4
10. Gawrilow, E., Joswig, M.: Polymake: a framework for analyzing convex polytopes. In: Kalai, G., Ziegler, G.M. (eds.) Polytopes—Combinatorics and Computation, pp. 43–74. Birkhäuser, Basel (2000)
11. Guoxing, J., Yanfang, C.: An LBP-based multi-scale illumination preprocessing method for face recognition. J. Electron. **26**, 509–516 (2009)
12. He, S., Soraghan, J.J., OReilly, B.F., Xing, D.: Quantitative analysis of facial paralysis using local binary patterns in biomedical videos. IEEE Trans. Biomed. Eng. **56**, 2009 (1864–1870)
13. Heikkilä, M., Pietikäinen, M.: A texture-based method for modeling the background and detecting moving objects. IEEE Trans. Pattern Anal. Mach. Intell. **28**, 657–662 (2006)
14. Jin, H., Liu, Q., Tong, X.: Face detection using improved LBP under Bayesian framework. In: Proceedings of the 3rd International Conference on Image and Graphics, pp. 306–309 (2004)
15. Liao, S., Law, M.W.K., Chung, A.C.S.: Dominant Local Binary Patterns for texture classification. IEEE Trans. Image Process. **18**, 1107–1118 (2009)
16. De Loera, J.A.: The many aspects of counting lattice points in polytopes. Math. Semesterber. **52**, 175–195 (2005)
17. De Loera, J.A., Hemmeckeb, R., Tauzera, J., Yoshida, R.: Effective lattice point counting in rational convex polytopes. J. Symb. Comput. **38**, 1273–1302 (2004)
18. Lucieer, A., Stein, A., Fisher, P.: Multivariate texture-based segmentation of remotely sensed imagery for extraction of objects and their uncertainty. Int. J. Remote Sens. **26**, 2917–2936 (2005)

19. Mäenpää, T., Pietikäinen, M.: Texture analysis with Local Binary Patterns. In: Chen, C.H., Pau, L.F., Wang, P.S.P. (eds.) Handbook of Pattern Recognition and Computer Vision, 2nd edn., pp. 197–216. World Scientific, Singapore (2005)
20. Mäenpää, T., Turtinen, T., Pietikäinen, M.: Real-time surface inspection by texture. Real-Time Imaging **9**, 289–296 (2003)
21. Mäenpää, T., Ojala, T., Pietikäinen, M., Maricor, S.: Robust Texture Classification by Subsets of Local Binary Patterns. In: Proceedings of the International Conference on Pattern Recognition, Barcelona (Spain), September 2000 (2000)
22. Motzkin, T.S., Raifa, H., Thompson, G.L., Thrall, R.M.: The Double Description Method, vol. 2. Princeton University Press, Princeton (1953)
23. Nanni, L., Lumini, A.: Local binary patterns for a hybrid fingerprint matcher. Pattern Recognit. **41**, 3461–3466 (2008)
24. Nanni, L., Lumini, A., Brahnam, S.: Local binary patterns variants as texture descriptors for medical image analysis. Artif. Intell. Med. **49**(2), 117–125 (2010)
25. Ojala, T., Pietikäinen, M., Harwood, D.: A comparative study of texture measures with classification based on feature distributions. Pattern Recognit. **29**, 51–59 (1996)
26. Ojala, T., Pietikäinen, M., Mäenpää, T.: Multiresolution gray-scale and rotation invariant texture classification with Local Binary Patterns. IEEE Trans. Pattern Anal. Mach. Intell. **24**, 971–987 (2002)
27. Petrou, M., García Sevilla, P.: Image Processing. Dealing with Texture. Wiley-Interscience, New York (1982)
28. Rosenfeld, A., Kak, A.C.: Digital Picture Processing. Academic Press, San Diego (1982)
29. Shan, C., Gong, S., McOwan, P.W.: Facial expression recognition based on local binary patterns: A comprehensive study. Image Vis. Comput. **27**, 803–816 (2009)
30. Shulman, N., Feder, M.: The Uniform Distribution as a Universal Prior. IEEE Trans. Inf. Theory **50**, 1864–1870 (2004)
31. Sørensen, L., Shaker, S.B., De Bruijne, M.: Quantitative analysis of pulmonary emphysema using local binary patterns. IEEE Trans. Med. Imaging **29**, 559–569 (2010)
32. Stanley, R.P.: Enumerative Combinatorics, vol. 1. Cambridge University Press, Cambridge (1997)
33. Tajeripour, F., Kabir, E., Sheikhi, A.: Fabric defect detection using modified local binary patterns. EURASIP J. Adv. Signal Process. (2008). doi:10.1155/2008/783898
34. Takala, V., Pietikäinen, M.: Multi-object tracking using color, texture and motion. In: Proceedings of the Seventh IEEE International Workshop on Visual Surveillance, Chicago, (USA), June 2007 (2007)
35. Tuceryan, M., Jain, A.K.: Texture analysis. In: The Handbook of Pattern Recognition and Computer Vision, 2nd edn. World Scientific, Singapore (1998)
36. van Herick, A.W.: Theoretical and computational methods for lattice point enumeration in inside-out polytopes. Master Thesis, San Francisco State University, San Francisco (USA), August 2007
37. Varma, M., Zisserman, A.: A statistical approach to material classification using image patch exemplars. IEEE Trans. Pattern Anal. Mach. Intell. **31**, 971–987 (2009)
38. Verdoolaege, S.: Barvinok: User Guide. Version: 0.30, March 2010. Available at http://freshmeat.net/projects/barvinok/
39. Xie, X., Mirmehdi, M.: A galaxy of texture features. In: Mirmehdi, M., Xie, X., Suri, J. (eds.) Handbook of Texture Analysis, pp. 375–406. Imperial College Press, London (2008)